COHEN WELLING BASES & $SO(2)$-EQUIVARIANT CLASSIFIERS USING TENSOR NONLINEARITY.

Anonymous authors
Paper under double-blind review

ABSTRACT

In this paper we propose autoencoder architectures for learning a Cohen-Welling (CW)-basis for images and their rotations. We use the learned CW-basis to build a rotation equivariant classifier to classify images. The autoencoder and classifier architectures use only tensor product nonlinearity. The model proposed by Cohen & Welling (2014) uses ideas from group representation theory, and extracts a basis exposing irreducible representations for images and their rotations. We give several architectures to learn CW-bases including a novel *coupling* AE architecture to learn a coupled CW-bases for images in different scales simultaneously. Our use of tensor product nonlinearity is inspired from recent work of Kondor (2018a). Our classifier has very good accuracy and we use fewer parameters. Even when the sample complexity to learn a good CW-basis is low we learn classifiers which perform impressively. We show that a coupled CW-bases in one scale can be deployed to classify images in a classifier trained and tested on images in a different scale with only a marginal dip in performance.

1 INTRODUCTION

A fundamental problem in vision is understanding how the human eye sees objects and images as being the same even when they undergo transformations. To obtain such a behaviour in a machine learning set-up, a natural idea is to construct representations of the object which remain the same even when the object undergoes transformations. This 'handcrafting' of representations of the object *invariant* to transformations was the preferred method of the vision community for a long time. Since the pathbreaking achievements of modern convolutional neural networks beginning with the seminal work of Krizhevsky et al. (2012) the focus has changed - the interest is more now on developing algorithms that learn to construct these invariant representations from transformed examples.

Goodfellow et al. (2009) were among the first to address the question of invariance in deep networks. Cohen & Welling (2014) were among the first to use representation theory of compact Lie groups to give it a sound mathematical framework. Developing on on ideas from earlier works of Rao & Ruderman (1999) and Sohl-Dickstein et al. (2010) on the Lie group model, Cohen and Welling build a model for the abelian group of transformations $SO(2)$, the group of rotations of the plane. Using their model they learn a nice basis for the underlying vector space in which the images sit, which allows them to read off the types and multiplicities of the irreducible representations of $SO(2)$ which occur in images under rotations. In this *basis exposing irreducible representations*[1], the action of an element of $SO(2)$ on an image is very easy to describe. From projections of images onto this basis,[2] Cohen and Welling obtain features of images which they use for classification.

A number of experts attribute the impressive performance of modern deep convolutional networks (CNN's) to the fact that more complex and abstract features are learned as one moves down the network. Nonlinearity seems to be essential to learn such features. Deep networks achieve their nonlinearity by the use of activation functions such as RELU, Krizhevsky et al. (2012). Convolution networks are by design invariant to translations. Given the incredible success of these deep networks the quest is now to build networks that have invariance to a larger group of symmetries.

[1] a phrase from Cohen & Welling (2014)
[2] hereafter called a CW-basis

In Bruna & Mallat (2013) the authors show that the first two layers of the scattering network yield a powerful representation of images which is invariant to geometric transformations. Gens & Domingos (2014) proposed deep symmetry networks, symnets, that form feature maps over large symmetry groups. They showed that Symnets over the affine group have smaller sample complexity. More recently, Group Convolutional Networks (GCNN's) were introduced in Cohen & Welling (2016a) and Harmonic nets were introduced by Worrall et al. (2017). Both GCNN's and Harmonic nets are designed to learn representations of images invariant to a larger set of symmetries than translations. The resulting networks perform impressively - the error rate reported by GCNN's on the MNIST-rot data set is only 2.28%. Harmonic nets are now the state of the art on MNIST-rot with a reported 1.62% error.

More recently Cohen & Welling (2016b) introduced Steerable CNN's based on more sophisticated ideas from group representation theory. This puts constraints on the network weights and architecture, and results in a reduction in the number of parameters to be learned. Steerable CNN's were shown to outperform ResNets He et al. (2016) and achieve state of the art results on CIFAR 10,100.

In both GCNN's as well in in steerable CNN's equivariance to the symmetries of a group G is achieved by a generalized form of convolution. The standard convolution in CNN's is replaced with the convolution of functions from G to $\mathbb{C}$. Kondor & Trivedi (2018b) proved the converse - they showed that any neural network which achieves equivariance with respect to the action of a group G, necessarily implements such a generalized convolution of functions on G.

If one were to factor out depth, it appears that it is the nonlinearity of the activation functions used in deep networks that is responsible for their impressive performance. But nonlinear functions like RELU are mathematically hard to analyze. It would be nice to design networks which construct features, just as deep networks seem to do in their various layers, with more mathematically amenable activation functions. This is the first motivation of this study.

Our other motivation comes from what is done in Pattern theory, Mumford (1997) where, to learn images, a stochastic model of the images to be learned is first built. To build a stochastic model of natural images it is important to view images under different scales simultaneously (Mumford (1997, Chapter 6)). Scattering networks address this issue because they use a wavelet basis for images.

This leads us to the following motivating questions. Can one use a mathematically amenable nonlinearity like tensor-product nonlinearity to design neural nets for image classification, leveraging ideas from group representation theory? How does one obtain complex abstract features from simple features using such a nonlinearity? Does it help to view images under different scales simultaneously to build such neural nets?

In this paper we make a modest attempt to answer such questions. We combine ideas from Cohen & Welling (2014) and Kondor (2018a), and design neural networks leveraging notions of tensor products of group representations. We decouple the classification process in two steps - first discover Cohen-Welling bases and then deploy them to train classifiers using ideas from Kondor.

2 PRELIMINARIES

We start with some definitions which set the stage for the work of Cohen & Welling (2014). Let G be a group and let V be a finite-dimensional vector space over a field - we will always assume that the underlying field is the field of complex numbers $\mathbb{C}$, or the field of real numbers $\mathbb{R}$. Let $GL(V)$ denote the group of invertible linear transformations of V.

Definition 1 *We say G acts on V if there is a group homomorphism ρ from G to $GL(V)$.*

So $g \in G$ acts on a vector $v \in V$ by sending v to $\rho(g)v$. If V has dimension d, then with respect to a basis of V, $\rho(g)$ is given by a $d \times d$ matrix. The action is then given by multiplying $\rho(g)$ with v. We denote this by $g \cdot v$.

Definition 2 *We say a subspace W of V is G-invariant under the action of G if for all $g \in G$ and all $w \in W$, $\rho(g)w \in W$. If V has no proper subspace which is G-invariant we say V is irreducible. The restriction of the action of G to a G-invariant subspace W is called a subrepresentation.*

Suppose V has an invariant subspace W, and we can also find a G-invariant subspace U such that $W \oplus U = V$. Then one can choose a basis of W and of U giving us a basis of V. In this basis each $\rho(g)$ will be a block diagonal matrix consisting of two blocks of size $dim(W)$ and $dim(U)$. For certain groups (called reductive groups) there is always such a U, and the group of rotations of the plane, $SO(2)$, is an example of such a group. For reductive groups we can continue this process till we have a decomposition of V into irreducibles, $V = U_1 \oplus U_2 \oplus \ldots \oplus U_k$.

Definition 3 *If V and W are representations of a group G, a G-morphism (aka a G-equivariant map) from V to W is a linear map ϕ from V to W such that $\phi(g \cdot v) = g \cdot \phi(v)$.*

If V and W are vector spaces over complex numbers Schur's lemma, Serre (1977), places restrictions on the dimension of the space of G-morphisms. First, if V and W are irreducible representations of G, Schur's lemma states the space of G-morphisms between them is either one dimensional (i.e every G-morphism between them is given by a scalar matrix) or zero dimensional (i.e the zero morphism is the only G-morphism between them). This allows us to group irreducible representations into types, with two of them being of the same type when there is a nonzero G-morphism between them.

Given a decomposition of a vector space with a G-action into a direct sum of irreducibles as above, we collect all irreducibles of the same type together and write $V = m_1 S_{t1} \oplus m_2 S_{t2} \cdots \oplus c_k S_{tk}$. Here tk is an indexing set for types, S_{ti} is an irreducible G-representation of type ti, and S_{ti} and S_{tj} are of different types when $i \neq j$. We then say S_{ti} occurs in V with multiplicity m_i in the decomposition of V. Now assuming that $V = \oplus_{i=1}^{i=k} m_i S_{ti}$ and $W = \oplus_{i=1}^{i=k} n_i S_{ti}$, it follows that the dimension of the space of G-morphisms between V and W is $\sum_i m_i n_i$.

Cohen & Welling (2014) considered the problem of supervised learning of images under the group $SO(2)$. Viewing an $N \times N$ image as an N^2 dimensional vector, an element of $SO(2)$ acts on an N^2 dimensional vector by taking the vector representing the image to the vector representing the rotated image. $SO(2)$ is an abelian group (rotating an image by θ_1 and then by θ_2 or rotating it first by θ_2 and then θ_1 yields the same image). Hence, over complex numbers, the irreducible representations of $SO(2)$ are one-dimensional (see, Kanatani (1990)). When the underlying space is a real vector space (as was considered in Cohen & Welling (2014)), the types are parametrized by nonnegative integers n (over complex numbers the irreducible representations are parametrized by all integers). The irreducible representation corresponding to type $n = 0$, S_0 is one-dimensional and is an invariant under $SO(2)$. For $n > 0$, the irreducible representation S_n is two dimensional (over complex numbers this splits into two one-dimensional representations parametrized by $\pm n$).

It follows, say, from Kanatani (1990, 2.3.7, 2.4.7) that there is a change of basis of the underlying vector space V with respect to which the action of the rotation group is given by a block diagonal matrix D with blocks of size 1 and 2. It is easy to describe these blocks. Blocks of size 1 correspond to invariants, of type $n = 0$, and have entry 1. The number of such blocks is called the multiplicity of the space of invariants in V. The block corresponding to nonzero n is the elementary rotation matrix $\begin{bmatrix} \cos(n\theta) & -\sin(n\theta) \\ \sin(n\theta) & \cos(n\theta) \end{bmatrix}$. It follows that the number of such blocks is the multiplicity of irreducible type n in V.

So there exists an $N \times N$ orthogonal matrix W and a diagonal matrix D, as above, with the property that when an image x is rotated by θ the transformed image is given by $WDW^t x$. In Cohen & Welling (2014), the authors address the question of determining the matrix W and the multiplicity with which a given n appears. The input is collection of pairs (x, y), of an image x and it's transformation y when it is rotated by an unknown angle θ. The authors find W using expectation-maximization over an interesting prior. The W their algorithm outputs is almost always a small subspace of the image space, spanning only some of the irreducible subspaces (similar to an SVD procedure which just outputs only the top few singular vectors). So strictly speaking we should be calling this a CW-subbasis since it may not span the image space, but we ignore this technicality.

An image x is then projected onto the W constructed and the vector of projected values, $W^T x$, were used by Cohen and Welling as elementary features of the image for classification.

Recently Kondor (2018a) proposed a neural network for learning the behaviour and properties of complex many-body physical systems.The neurons in this system operate entirely in the Fourier space.The neurons compose activations following Schur's lemma, thereby ensuring that the activations are covariant to rotations.

We pose our motivating questions more precisely using the language of Cohen-Welling.

1. Can we obtain a CW-basis of images and their rotations using tensor product nonlinearity?
2. How can elementary features obtained using a CW-basis be combined to get more complex abstract features for building good classifiers?
3. Can one discover CW-bases of images in two scales in tandem, with one influencing the discovery of the other? Do such *coupled* bases perform better in classification? Can one use these *coupled* CW-bases interchangeably?

Our contributions We give an affirmative answer to all the questions. We give several architectures to construct such bases. We use Kondor's framework to construct a classifier which takes elementary features and combines them using simple ideas from the representation theory of $SO(2)$.[3] We give a simple coupled autoencoder architecture which answers question 3 above - we use tensor product nonlinearity crucially. While such bases are not better at classification we show that they can be interchangeably used with a marginal drop in performance.

2.1 Notions from representation theory

To describe our set up and explain our experiments we will need a few more notions from representation theory. Throughout we will assume that the underlying group G is a reductive group, in fact the reader may think of G as $SO(2)$.

If V is a representation of a group G then the dual vector space V^* acquires a natural G action given by $(g \cdot f)(v) = f(g^{-1}v)$, for $f \in V^*, v \in V$. If V, U are representations of a reductive group then $V \otimes U$ is a representation of the product group $G \times G$. Furthermore, since G is a subgroup of $G \times G$ under the diagonal embedding (g mapping to (g, g)), $V \otimes U$ is a representation of G. And by what we described above $V \otimes U$ splits into a direct sum of irreducible representations identified by their types and multiplicities. It follows that the tensor algebra $T(V) = \oplus_i V^{\otimes i}$ of V is an (infinite dimensional, algebraic) representation of G.

Remark 4 *When G is $SO(2)$ and $0 \neq i < j$ then $S_i \otimes S_j$ splits into a direct sum $S_{i+j} \oplus S_{j-i}$. When $i = 0$ $S_i \otimes S_j$ is isomorphic to S_j, (Kanatani (1990)).*

To make precise the question about coupled bases and features from a coupled bases we need one more definition.

Definition 5 *We say G-representations V and W are coupled if W is the image of a G-morphism of a finite dimensional subrepresentation of the tensor algebra of V, and V is the image of a G-morphism of a finite dimensional subrepresentation of the tensor algebra of W.*

The above definition is equivalent to requiring that W can be realized as a subrepresentation (or a quotient) of the tensor algebra of V and V can realized as a subrepresentation (or a quotient) of the tensor algebra of W.

Definition 6 *Let V be the vector space of 14×14 images and let W be the vector space of 28×28 images. Assume the rotation group $SO(2)$ acts on both. We say a Cohen-Welling basis X of V is coupled to a Cohen-Welling basis Y of W if the vector space dual of the subspace spanned by X (with its $SO(2)$-action) is coupled to the vector space dual of the subspace spanned by Y.*

Recall that by projecting an image on to a CW-basis we get elementary features of the image which are used for classification. These elementary features are elements of the vector space dual of the space spanned by the CW-basis, hence the need for the word dual in the above definition. Motivated by the above definition we say features obtained from coupled CW-bases are *coupled features*.

The definition above is motivated by our question of whether one can build CW-bases in two different scales with one influencing the discovery of the other and vice-versa. Our definition suggests

[3] As we were getting this write up ready we were pointed to some recent work of Kondor et al. (2018c) - the authors do similar work, but use the rotation group $SO(3)$ - for completeness we have included their results in Table 1.

that in order to generate coupled CW-bases we will need to view the images at different scales simultaneously, and use tensor product nonlinearity to generate them, thereby forcing the influence we are looking for.

Remark 7 *One last remark is in order before we describe our setup and experiments. We are working over the field of real numbers, so Schur's lemma does not apply in our situation. Nevertheless when we look for $SO(2)$-morphisms between two irreducible vector spaces with an $SO(2)$-action we will assume that the morphisms are of the kind Schur's lemma dictates - either we have no morphism or the morphism is given by a scalar matrix rId, r a real number and Id being the identity matrix.*

3 EXPERIMENTS AND RESULTS

We use the notation W_ℓ for a CW-basis of images of size $\ell \times \ell$. So W_ℓ is a $\ell^2 \times d$ matrix for some d (usually smaller than l^2). Recall that if W_ℓ is a CW-basis is is easy to describe how to rotate an $\ell \times \ell$ image x by an angle θ - it is the ℓ^2-size vector $W_\ell D_\ell(\theta) W_\ell^T x$, where D_ℓ is the block diagonal matrix described in section 2, of size the cardinality of W_ℓ. If a column of W_ℓ represents a basis vector which is invariant the corresponding block is 1 and if a pair of columns in W_ℓ is a basis for an irreducible representation of type n, the block in D for this pair is the elementary rotation matrix described in section 2. When there is no confusion we will ignore the subscripts.

We give three neural net architectures to discover CW-bases of images. To construct a CW-basis we use MNIST-rot images as inputs. In Cohen & Welling (2014) inputs are images generated using a standard Gaussian distribution with mean zero and images are rotated by an angle between 0 and 2π.

3.1 LEARNING CW-BASES

1. **An autoencoder(AE) architecture.** The autoencoder(AE) architecture is given as an Algorithm(see Alogrithm 1). An equivalent block diagram with explanation in given in the appendix (see figure 6).

Algorithm 1: AutoEncoder

Input: $X_i \in \mathbb{R}^{784}, i \in \{1, 2, \dots\}$
Hyper-parameters : a_j, b_j, β
Let $d_a = a_0 + \sum_{j=1} 2 \times a_j \quad ; \qquad d_b = b_0 + \sum_{j=1} 2 \times b_j$
Output: $W_{28} \in \mathbb{R}^{784 \times d_a}$
Output: $\phi \in \mathbb{R}^{d_b \times d_a}$ `// Equivariant linear map (Block diagonal`
Output: $\psi \in \mathbb{R}^{d_a \times (d_b + {d_b}^2)}$ `// matrix) as dictated by Remark 7`

for $i = 1, 2, \dots$ **do**
  $\theta_i \in U[0, 360)$ `// Choosen uniformly at random`
  $Y_i =$ Rotate (X_i, θ_i) `// Rotate is the standard image rotation`
  $\hat{Y}_i = W_{28}^T Y_i$
  $Z_i = \psi(\phi(\hat{Y}_i) \otimes \phi(\hat{Y}_i) \oplus \phi(\hat{Y}_i))$
  $\hat{X}_i = D(-\theta_i) Z_i$ `// Unrotate the image`
end
$L = \sum_i |X_i - \hat{X}_i|_2^2$ `// Loss function`
$W_{28}, \phi, \psi = \min_{W_{28}, \phi, \psi} (L + \beta |W_{28}^T W_{28} - Id_{d_a \times d_a}|_1)$
return W_{28}, ϕ, ψ

Choosing $[10, 5, 5, 5, 5, 4, 4, 4, 4, 4, 3, 3, 3, 3, 3, 2, 2, 2, 2, 2, 1, 1, 1, 1, 1]$ as our multiplicities for the a_i's and $[8, 4, 4, 4, 4, 3, 3, 3, 3, 3, 2, 2, 2, 2, 2, 1, 1, 1, 1, 1]$ for the b_i's, we learn a really sharp W_{28} as shown in appendix Figure 7.

2. **Coupled Autoencoder(CAE) architecture**. In this setup, Figure 1, we learn W_{14} and W_{28} in tandem. We feed both, an image X and a scaled down version of the image x to the network.

The network on top takes x and produces $\hat{X}$ a 28x28 image. The bottom network takes X and produces $\hat{x}$ a 14x14 image. The two networks are connected and we use the same W_{28}, and W_{14} in the top and bottom layer. Hyperparameters are multiplicities of $SO(2)$-irreducible representations in W_{28} and W_{14}. We learn the W_{14}, W_{28} and two $SO(2)$-equivariant maps ϕ and ψ. The bottom network takes X, rotates it by θ and projects the resulting Y on the current W_{28}, to get $\hat{Y} = W_{28}^T Y$. Applying ϕ we get $\phi(\hat{Y})$. We unrotate $\phi(\hat{Y})$ using $D_{14}(-\theta)$ to get z. We generate a 14x14 image using current W_{14} to get $\hat{x} = W_{14}z$. The top network takes x rotates it by the same θ. This is projected onto the current W_{14} to get $\hat{y}$. We apply ψ to $\hat{y} \oplus (\hat{y} \otimes \hat{y})$ and unrotate the resulting vector using $D_{28}(-\theta)$ to get Z. We use the current W_{28} to get $\hat{X} = W_{28}Z$. We minimize the reconstruction error $|X - \hat{X}|^2 + |x - \hat{x}|^2$.

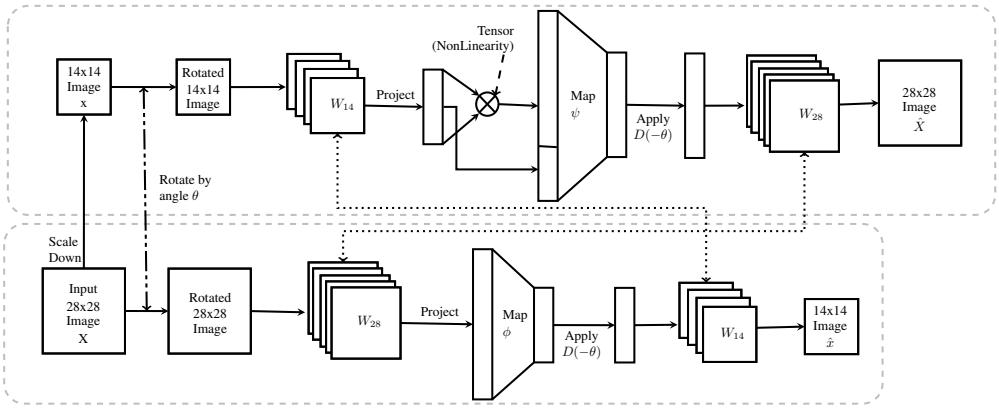

Figure 1: Coupled autoencoder architecture (CAE)

3 **Bootstrapping W_{14} to W_{28}, W_{28} to W_{14}.** In this experiment we start with a known W_{14} obtained using experiment 1 for 14x14 images, to learn a W_{28}. The setup to go from W_{14} to W_{28} is exactly the part of the network in Figure 1 going from X to $\hat{X}$ along the top. The hyperparameters are the multiplicities of $SO(2)$-irreducible representations in W_{28}. We learn the $SO(2)$-equivariant ψ and W_{28} by minimizing $|X - \hat{X}|^2$. Similarly starting with a known W_{28} we can learn W_{14} by following the path in Figure 1 from x to $\hat{x}$ along the bottom.

3.2 Classification using the learned CW-basis

Figure 2 shows a 2 layer classification network for 28×28 images - this can be extended to any number of layers and other image sizes. This is a logical extension of the auto encoder network (Experiment 1). It is a CNN in Fourier domain using tensor product nonlinearity. Assume the dimension of W_{28} is d_W. We project the image x onto W_{28} to get $W_{28}^T x$. Let L_1 be a vector space with an $SO(2)$-action - hyperparameters are multiplicities l_{1j} of irreducibles $SO(2)$-representations S_j in L_1. We learn an $SO(2)$-equivariant map ϕ_1 from the image space of W_{28}^T to L_1. The $SO(2)$-decomposition of $l_1 = \phi_1(W_{28}^T x) \oplus (\phi_1(W_{28}^T x) \otimes \phi_1(W_{28}^T x))$ is computed. This is the input to the next layer. There we choose a vector space L_2 with a $SO(2)$-action which splits into irreducibles S_j with multiplicities l_{2j} (hyperparameters). We learn a second $SO(2)$-equivariant map ϕ_2 from $L_1 \oplus (L_1 \otimes L_1)$ to L_2 and compute $\phi_2(l_1)$. We compute the tensor product of $\phi_2(l_1)$ with itself and produce $l_2 = \phi_2(l_1) \oplus (\phi_2(l_1) \otimes \phi_2(l_1))$. This is the input to the next layer. So we learn as many $SO(2)$-equivariant maps as there are layers. In the final layer, l_f is projected onto the invariant space (the multiplicity of S_0 in $L_f \oplus (L_f \otimes L_f)$ and fed to a soft max classifier.

3.3 Results

1. **Construction of CW-basis**

   We construct CW-basis W_{14} for 14×14 images and CW-basis W_{28} for 28×28 in the various architectures. We evaluate these bases in terms of image reconstruction error (MSE). We also used rotation reconstruction error by comparing with scikits-image rotation. Figure 3 and Figure 4 shows graphs of the error functions for W_{28} constructed in an AE architecture and a CAE

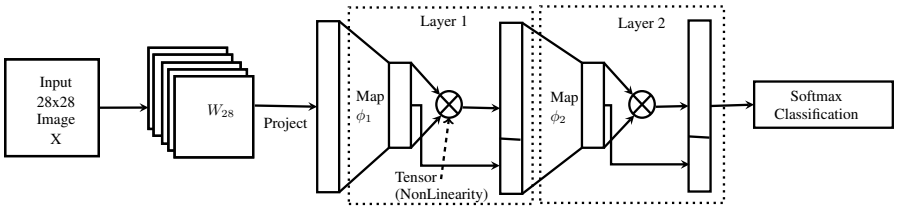

Figure 2: Classification network

as a function of the number of samples given to the AE and CAE architectures to learn the W_{28}. As the figures show, even when the number of samples is as small as 50, we discover CW-bases which are good at rotation and also reconstruction in both AE and CAE architectures.

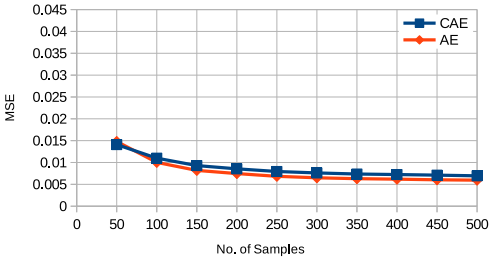

Figure 3: MSE - Reconstruction of images

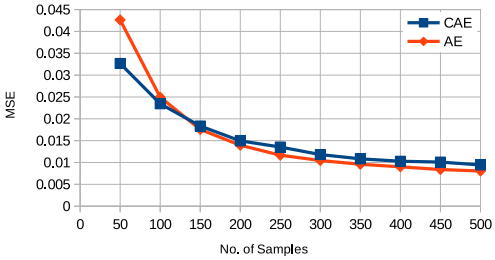

Figure 4: MSE - Rotation of images

2. **Results on Classification** In Figure 5 we plot the accuracy of these various W_{28} obtained above when deployed for classification. Our classifier was trained and tested on MNIST-rot. We plot the accuracy of the classifier as a function of the number of samples used to construct the CW-bases. When the number of samples is as low as 50 a CAE-W_{28} performs better than an AE-W_{28}. Beyond 100 samples the difference is insignificant. The plots using a bootstrapping CW-basis are not given as they were very similar to that of the AE.

   In Table 1 we give the accuracy of our classifier when trained and tested on combinations using MNIST(NR) and MNIST-rot(R). The R/NR column for example denotes the accuracy when trained on MNIST-rot and tested on MNIST. For comparison we use Planar, Spherical CNN accuracies given in Cohen et al. (2018). We also compare with FFS2CNN, (see Kondor et al. (2018c)).

   The fourth row shows the accuracy of our classifier that used a CAE-W_{28}. This was obtained using CAE architecture which was given 12000 training samples of MNIST-rot to discover the W_{28}. Our classifier performs better in all the scenarios.

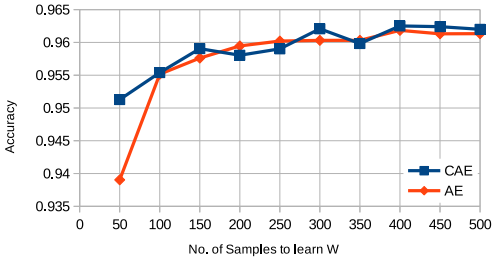

Figure 5: Classification accuracy

Coupling interchangeability To test how coupled the CAE-W_{28} and CAE-W_{14} are, we did the following experiment - the classifier trained in row 4 with CAE-W_{28} was presented with down sized 14x14 images for classification. No additional training was done. Instead we use the top half of the coupling network from Figure 1 - given a test image y we compute $\hat{y} = W_{14}^T y$ using

the CAE-W_{14}. Then $\psi((\hat{y} \otimes \hat{y}) \oplus \hat{y})$ is fed to the trained classifier of row 4. These results are reported in row 5 as [28/14 Tensor].

For comparison we took the 14x14 images and scaled them up to 28x28. And then fed them to the trained classifier of row 4. These results are reported in Row 6 as [28/14 Scale]. Using CAE-W_{14} is better, indicating that a coupled bases retains scale information well.

We repeated the same experiment when the coupled network is given only 500 samples to learn the CAE-W_{28} and CAE-W_{14}. As row 8 shows, performance is till very good.

Table 1: MNIST - Accuracies - rotated, unrotated combinations

	Samples used to learn W	R / R	R / NR	NR / NR	NR / R
Planar [1]	-	0.23	-	0.98	0.11
Spherical CNN [1]	-	0.95	-	0.96	0.94
FFS2CNN [2]	-	0.958	-	0.96	0.9586
Ours	12000	0.968	0.968	0.976	0.985
28 / 14 Tensor	12000	0.962	0.964	0.972	0.976
28 / 14 Scale	12000	0.949	0.957	0.944	0.922
Ours	500	0.962	0.963	0.973	0.981
28 / 14 Tensor	500	0.956	0.958	0.964	0.970
28 / 14 Scale	500	0.945	0.953	0.938	0.917

[1] Values as reported in Table 1 of Cohen et al. (2018)
[2] Values as reported in Kondor et al. (2018c)

3.4 Implementation

We implement our autoencoders and classifiers as neural nets in Python (TensorFlow) and used Adam optimizer. For the classifier we use a 3 layer network with 28K parameters. In comparison Spherical networks use 58K and FFS2CNN 342K.

4 Conclusion and future work

We answer in the affirmative all our motivating questions - we design architectures which learn CW-bases and classify using only tensor product nonlinearity. We obtain some state of the art results. It appears that coupling bases do retain scale information and can be interchangeably used for classification albeit with a small drop in performance. There is no appreciable advantage in using coupled bases for classification excepting when the bases are learned using small samples of inputs.

Tensor product nonlinearity allows us to decouple the classification problem in two steps. One advantage of decoupling the process is that the basis can be obtained offline. Our ideas can be extended to other groups. We have begun experiments with the action of the S_n on images.

We are testing our architectures on CIFAR-10. One issue we run into when using architectures with a lot of depth, is that accuracy increases and then drops. A similar issue is resolved in RES-nets He et al. (2016) by computing residual functions. In ongoing work we proceed similarly since the residual function is $SO(2)$-equivariant.

Robustness of classifiers to noise is an active area of research, (see Goodfellow et al. (2018)). We believe our classifiers built from bases learnt in a CAE architecture should be robust to noise - our belief comes from the fact that coupling bases can be used interchangeably. We plan to investigate this.

Acknowledgements

The authors would like to thank Infosys foundation for a generous grant.

REFERENCES

Joan Bruna and Stéphane Mallat. Invariant scattering convolution networks. *IEEE transactions on pattern analysis and machine intelligence*, 35(8):1872–1886, 2013.

Taco S. Cohen and Max Welling. Learning the Irreducible Representations of Commutative Lie Groups. In *Proceedings of the 31st International Conference on Machine Learning*, volume 32, pp. 1755–1763, February 2014. ISBN 9781634393973.

Taco S. Cohen and Max Welling. Group Equivariant Convolutional Networks. *Proceedings of The 33rd International Conference on Machine Learning*, 48, feb 2016a.

Taco S Cohen and Max Welling. Steerable cnns. *arXiv preprint arXiv:1612.08498*, 2016b.

Taco S. Cohen, Mario Geiger, Jonas Khler, and Max Welling. Spherical CNNs. In *International Conference on Learning Representations*, 2018.

Robert Gens and Pedro M Domingos. Deep symmetry networks. In *Advances in neural information processing systems*, pp. 2537–2545, 2014.

Ian Goodfellow, Honglak Lee, Quoc V Le, Andrew Saxe, and Andrew Y Ng. Measuring invariances in deep networks. In *Advances in neural information processing systems*, pp. 646–654, 2009.

Ian J. Goodfellow, Patrick D. McDaniel, and Nicolas Papernot. Making machine learning robust against adversarial inputs. *Commun. ACM*, 61(7):56–66, 2018. doi: 10.1145/3134599.

Kaiming He, Xiangyu Zhang, Shaoqing Ren, and Jian Sun. Deep residual learning for image recognition. In *2016 IEEE Conference on Computer Vision and Pattern Recognition, CVPR 2016, Las Vegas, NV, USA, June 27-30, 2016*, pp. 770–778, 2016. doi: 10.1109/CVPR.2016.90.

Kenichi Kanatani. Shape from texture. In *Group-Theoretical Methods in Image Understanding*, pp. 327–355. Springer, 1990.

R. Kondor, Z. Lin, and S. Trivedi. Clebsch-Gordan Nets: a Fully Fourier Space Spherical Convolutional Neural Network. *ArXiv e-prints*, 2018c.

Risi Kondor. N-body networks: a covariant hierarchical neural network architecture for learning atomic potentials. *arXiv preprint arXiv:1803.01588*, 2018a.

Risi Kondor and Shubhendu Trivedi. On the generalization of equivariance and convolution in neural networks to the action of compact groups. *arXiv preprint arXiv:1802.03690*, 2018b.

Alex Krizhevsky, Ilya Sutskever, and Geoffrey E Hinton. Imagenet classification with deep convolutional neural networks. In *Advances in neural information processing systems*, pp. 1097–1105, 2012.

David Mumford. Pattern theory: a unifying perspective. In *Fields Medallists' Lectures*, pp. 226–261. World Scientific, 1997.

Rajesh P N Rao and Daniel L Ruderman. Learning Lie groups for invariant visual perception. *Advances in Neural Information Processing Systems*, 816:810–816, 1999. ISSN 1049-5258. doi: 10.1.1.50.8859.

Jean-Pierre Serre. *Linear Representations of Finite Groups*, volume 42 of *Graduate Texts in Mathematics*. Springer New York, New York, NY, 1977. ISBN 978-1-4684-9460-0. doi: 10.1007/978-1-4684-9458-7.

Jascha Sohl-Dickstein, Jimmy C. Wang, and Bruno A Olshausen. An Unsupervised Algorithm For Learning Lie Group Transformations. *CoRR*, abs/1001.1:8, January 2010.

Nathaniel Thomas, Tess Smidt, Steven M. Kearnes, Lusann Yang, Li Li, Kai Kohlhoff, and Patrick Riley. Tensor field networks: Rotation- and translation-equivariant neural networks for 3d point clouds. *CoRR*, abs/1802.08219, 2018.

Daniel E Worrall, Stephan J Garbin, Daniyar Turmukhambetov, and Gabriel J Brostow. Harmonic networks: Deep translation and rotation equivariance. In *Proc. IEEE Conf. on Computer Vision and Pattern Recognition (CVPR)*, volume 2, 2017.

Appendices

A PROOFS

Here we prove that the bases obtained in the coupling architecture satisfy the definition of coupling. The proof is straightforward assuming that we have zero loss.

Let W_{28} and W_{14} be the final CW-bases learned. Following the bottom half of the network describing the coupling architecture, we see that under the morphism ϕ, the image space of W_{28}^T surjects onto the image space of W_{14}^T. Surjection follows since the dotted arrow going from W_{14} on the top to W_{14} below shows that we can start with any linear combination of the basis elements of W_{14} at the top and obtain it as the image of ϕ applied to an appropriate linear combination of basis elements of W_{28}. So the image space of W_{14}^T is isomorphic to a quotient of the image space of W_{28}^T. On the other hand following the top half of the network it is clear that ψ maps the image space of $W_{14}^T \oplus (W_{14}^T \otimes W_{14}^T)$ surjectively onto the image space of W_{28}^T. Surjectivity follows by reasoning as above. Hence the bases obtained in the coupling architecture satisfy definition 6.

B AUTOENCODER(AE) ARCHITECTURE

The schema is as given in Figure 6 (this architecture works for 14x14 images, 56x56 images). We use MNIST-rot images as input. The hyperparameters are multiplicities with which $SO(2)$ irreducible representations occur in MNIST-rot images viewed as vectors in a 784 dimensional vector space with an action of $SO(2)$. We choose nonzero multiplicities a_j for representations S_j with $0 \leq j \leq 24$ giving us a subspace of the image space of dimension $d_W = a_0 + \sum_j 2 * a_j$. We denote this subspace by W_{28} and learn a CW-basis also denoted W_{28}, a $784 \times d_W$ matrix. We initialize W_{28} randomly. We rotate a 28 x 28 image x by a random angle θ, to get y and project y onto W_{28} to get $\hat{y} = W_{28}^T y$. We learn an $SO(2)$-equivariant map ϕ from the image space of W_{28}^T to a vector space L with an $SO(2)$-action, with multiplicities (hyperparameters) b_j. Consider $\phi(\hat{y}) \in L$. Now $L \otimes L$ gets a natural $SO(2)$ action. Recall that the tensor product of an $SO(2)$ irreducible representation of type m and an $SO(2)$-irreducible representation of type type n yields irreducible representations of types $m+n$ and $m-n$, (w.l.o.g $m > n$). We use this to compute the decomposition of $\phi(\hat{y}) \otimes \phi(\hat{y})$. The last set of parameters to be learned are an $SO(2)$-equivariant map ψ from $L \oplus (L \otimes L)$ to the image space of W_{28}^T. Let $z = \psi(\phi(\hat{y}) \oplus (\phi(\hat{y}) \otimes \phi(\hat{y})))$. We unrotate z using $D(-\theta)$. Then we reconstruct the image $\hat{x} = W_{28} D(-\theta) z$ We expect this to be close to x so we minimize the reconstruction error $|\hat{x} - x|^2$ with a regularizer to ensure that $W_{28}^T W_{28}$ is identity.

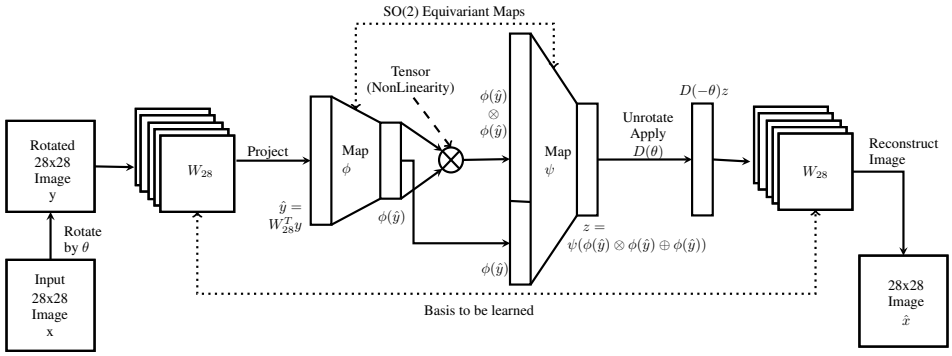

Figure 6: Autoencoder architecture (AE).

C VISUALIZATION OF CW BASIS

Figure 7 shows a few basis elements learned using AE schema.

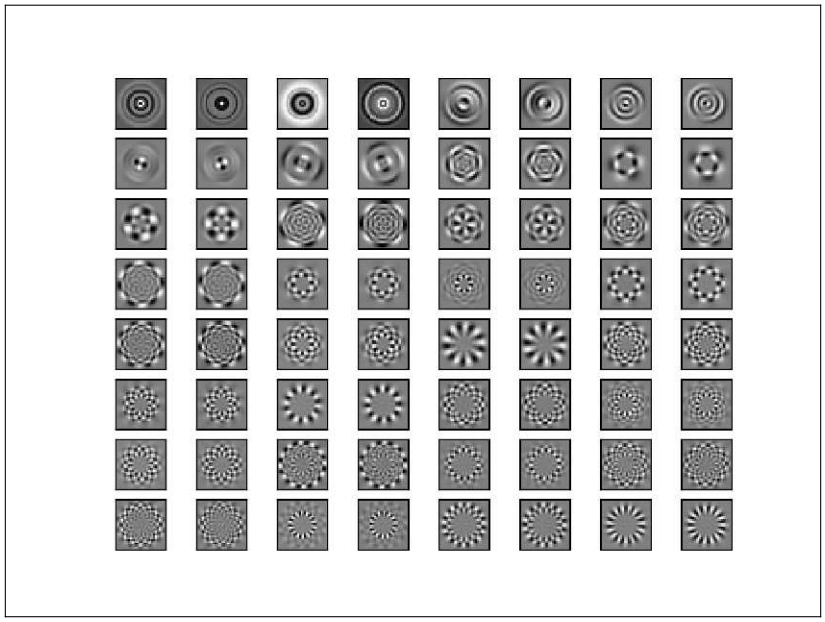

Figure 7: Basis for 28 x 28 images learned in experiment 1.

D TABLE WITH STATISTICS

Table 2 gives the mean accuracies in percentage and the standard deviation in paranthesis.

Table 2: MNIST - Accuracies - rotated, unrotated combinations

	Samples used to learn W	R / R	R / NR	NR / NR	NR / R
Ours	12000	96.73 (0.35)	96.90 (0.23)	97.68 (0.08)	98.48 (0.06)
28 / 14 Tensor	12000	96.17 (0.35)	96.51 (0.27)	97.10 (0.70)	97.51 (0.09)
28 / 14 Scale	12000	94.79 (0.59)	95.56 (0.55)	93.86 (0.87)	91.66 (1.36)
Ours	500	96.40 (0.09)	96.64 (0.06)	97.41 (0.09)	98.24 (0.05)
28 / 14 Tensor	500	95.78 (0.12)	95.98 (0.09)	96.53 (0.12)	97.03 (0.07)
28 / 14 Scale	500	94.37 (0.39)	95.34 (0.23)	92.67 (1.02)	89.62 (1.51)

E EXAMPLE

Let us see an example of how Z_i is calculated in Algorithm 1. Let d_a and d_b are as given in the Algorithm. $\phi \in \mathbb{R}^{d_b \times d_a}$ is a block diagonal matrix with blocks of sizes $b_0 \times a_0$, $2b_1 \times 2a_1, 2b_2 \times 2a_2, \ldots$ The first block has $(b_0 * a_0)$ entries ,the second block has $(b_1 * a_1)$ entries with the following structure.

$$\begin{pmatrix} \alpha_{11} & 0 & \alpha_{12} & 0 & \ldots & \alpha_{a_1 1} & 0 \\ 0 & \alpha_{11} & 0 & \alpha_{12} & \ldots & 0 & \alpha_{a_1 1} \\ \alpha_{21} & 0 & \alpha_{22} & 0 & \ldots & \alpha_{a_1 2} & 0 \\ 0 & \alpha_{21} & 0 & \alpha_{22} & \ldots & 0 & \alpha_{a_1 2} \\ \vdots & \vdots & \vdots & \vdots & \ddots & \vdots & \vdots \\ \alpha_{1b_1} & 0 & \alpha_{2b_1} & 0 & \ldots & \alpha_{a_1 b_1} & 0 \\ 0 & \alpha_{1b_1} & 0 & \alpha_{2b_1} & \ldots & 0 & \alpha_{a_1 b_1} \end{pmatrix}$$

Let $\hat{Y}$ have the following multiplicities, $a = 2, 1, 2$ and $\phi(\hat{Y})$ have the following multiplicities $b = 0, 1, 1$. Hence $d_a = 8, d_b = 4$ and ϕ with arbitrary chosen values is given below.

$$\phi = \begin{pmatrix} 0 & 0 & 1 & 0 & 0 & 0 & 0 & 0 \\ 0 & 0 & 0 & 1 & 0 & 0 & 0 & 0 \\ 0 & 0 & 0 & 0 & 2 & 0 & 3 & 0 \\ 0 & 0 & 0 & 0 & 0 & 2 & 0 & 3 \end{pmatrix}$$

Boxes indicate the block for type 1 and type 2.

Let $\phi(\hat{Y}) = (p, q, r, s)^T$

When we tensor $(p, q)^T$ of type n with $(r, s)^T$ of type m (m > n), we get $(pr - qs, ps + qr)^T$ of type (m+n) and $(pr + qs, ps - qr)$ of type (m-n) (see Remark 4). In this example, when we tensor $\phi(\hat{Y})$ with itself, we get

$$\phi(\hat{Y}) \otimes \phi(\hat{Y}) = \begin{pmatrix} p^2 + q^2 \\ 0 \\ r^2 + s^2 \\ 0 \\ pr + qs \\ ps - qr \\ pr + qs \\ ps - qr \\ p^2 - q^2 \\ 2pq \\ pr - qs \\ ps + qr \\ pr - qs \\ ps + qr \\ r^2 - s^2 \\ 2rs \end{pmatrix}$$

with the following types : multiplicities - type 0 : 4, type 1 : 2, type 2 : 1, type 3 : 2, type 4 : 1.

During implementation we avoid duplicates and zeros and we use the following:

$$\phi(\hat{Y}) \otimes \phi(\hat{Y}) = \begin{pmatrix} p^2 + q^2 \\ r^2 + s^2 \\ pr + qs \\ ps - qr \\ p^2 - q^2 \\ 2pq \\ pr - qs \\ ps + qr \\ r^2 - s^2 \\ 2rs \end{pmatrix}$$

Also, $\phi(\hat{Y}) \otimes \phi(\hat{Y}) \oplus \phi(\hat{Y})$ after grouping the types, is given below:

$$\phi(\hat{Y}) \otimes \phi(\hat{Y}) \oplus \phi(\hat{Y}) = \begin{pmatrix} p^2 + q^2 \\ r^2 + s^2 \\ pr + qs \\ ps - qr \\ p \\ q \\ p^2 - q^2 \\ 2pq \\ r \\ s \\ pr - qs \\ ps + qr \\ r^2 - s^2 \\ 2rs \end{pmatrix}$$

The linear map $\psi \in \mathbb{R}^{d_c \times d_a}$ is similar to ϕ. Only the input and output multiplicities are different. In the example we have $c = (2, 2, 2, 1, 1)$ and $a = (2, 1, 2)$. A particular ψ with some fixed values is given below,

$$\psi = \begin{pmatrix} 1 & 2 & 0 & 0 & 0 & 0 & 0 & 0 & 0 & 0 & 0 & 0 & 0 & 0 \\ 3 & 4 & 0 & 0 & 0 & 0 & 0 & 0 & 0 & 0 & 0 & 0 & 0 & 0 \\ 0 & 0 & 5 & 0 & 6 & 0 & 0 & 0 & 0 & 0 & 0 & 0 & 0 & 0 \\ 0 & 0 & 0 & 5 & 0 & 6 & 0 & 0 & 0 & 0 & 0 & 0 & 0 & 0 \\ 0 & 0 & 0 & 0 & 0 & 0 & 7 & 0 & 8 & 0 & 0 & 0 & 0 & 0 \\ 0 & 0 & 0 & 0 & 0 & 0 & 0 & 7 & 0 & 8 & 0 & 0 & 0 & 0 \\ 0 & 0 & 0 & 0 & 0 & 0 & 9 & 0 & 10 & 0 & 0 & 0 & 0 & 0 \\ 0 & 0 & 0 & 0 & 0 & 0 & 0 & 9 & 0 & 10 & 0 & 0 & 0 & 0 \end{pmatrix}$$

And $Z_i = \psi(\phi(\hat{Y}) \otimes \phi(\hat{Y}) \oplus \phi(\hat{Y}))$